Journal of Science and Technology in Civil Engineering, HUCE (NUCE), 2022, 16 (4): 44–57

A NUMERICAL SOLUTION FOR SEISMIC RESPONSE PREDICTION OF BRIDGE PIERS WITH HIGH DAMPING RUBBER BEARINGS

Nguyen Anh Dung[a,*]

[a]*Civil and Industrial Construction Division, Thuyloi University, 175 Tay Son street, Dong Da district, Hanoi, Vietnam*

Article history:
Received 02/9/2022, Revised 27/9/2022, Accepted 28/9/2022

Abstract

The motion equation of a one-degree-of-freedom system when subjected to earthquakes is usually not solved by analytic methods. This problem can only be solved through the time step method, when integrating differential equations. This paper is devoted to presenting a numerical solution for a seismic analysis problem of a highway bridge pier with high damping rubber bearings under earthquakes. Based on time-stepping Newmark's method, a numerical solution is developed to predict the seismic responses of the piers. The iteration Newton-Raphson method is also applied in the problem for static analysis of this nonlinear system. The ground acceleration in the analysis is the type- II earthquake in JRA 2004 (Japan Road Association). Further-more, high damping rubber bearings are modeled by the two models: the bilinear design model and the rheology model proposed by authors. After that, the stress responses and the displacement responses of the pier are obtained by a program that is implemented in Matlab software. The comparison results obtained from the two models show that the seismic responses of the pier strongly depend on the modeling of the rubber bearings. This is the important note for engineers to design the earthquake resistance of bridges with high damping rubber bearings. The solution is also a useful tool for engineers to predict the seismic responses of bridge piers in the design procedure.

Keywords: numerical solution; motion equation; seismic responses; earthquakes; high damping rubber bearings.

https://doi.org/10.31814/stce.nuce2022-16(4)-04

1. Introduction

An analytical solution of the motion equation for practical problems such as predicting the responses of houses or bridges under earthquakes is not possible because the excitation – ground acceleration is complex to be analytically defined and is represented only numerically [1]. The only practical approach for such systems involves numerical time-stepping methods such as the Central difference method; Newmark's method. These numerical methods are very useful for predicting the dynamic response of nonlinear systems in engineering design practice.

Bridges are vital infrastructures, especially in emergencies like earthquakes. They are transportation lifelines of society for evacuation and aid when disasters occur. However, there were a lot of bridge structures that collapsed in earthquakes in Kobe, Japan (1995) and Northridge, USA (1994) [2]. Therefore, it is especially important to ensure the safety of bridges in the event of an earthquake.

*Corresponding author. *E-mail address:* dung.kcct@tlu.edu.vn (Dung, N. A.)

Recently, the base isolator has become a technique solution of construction in highly seismic areas [3]. Among many types of isolators, laminated rubber bearings are very popular in the world. The laminated rubber bearings are three types: lead rubber bearings; nature rubber bearings; and high damping rubber bearings (HDRB). HDRB are used widely in Japan due to their large strength and high damping. Although HRDB has been used for several decades, the design analysis of structures with HDRB is still a complicated problem because the mechanical behavior of HDRB is quite complex.

In this paper, a numerical solution based on Newmark's method is developed to predict the seismic responses of the bridge piers using HDRB under the type- II earthquake in JRA 2004 [4]. The Newton-Raphson method is also employed in this calculation for static analysis of the nonlinear system. There are some algorithms that are proposed and implemented in Matlab software [5]. Two models are used for HDRB for the purpose of comparison. The comparison results show that the seismic responses of bridges strongly depend on the modeling of HDRB. This is the important note for engineers to design bridge structures with HDRB.

2. A seismic analysis problem of a bridge pier used HDRB under earthquakes

A multi-span continuous bridge in [6] is used in this analysis. The bridge is the continuous reinforced concrete (RC) deck-steel girder bridge isolated by HDRB provided at top of the RC piers. The isolated bearings are positioned between the steel girders and top of the piers. The geometric dimensions of HDRB in the prototype bridge are given in Table 1.

Table 1. Properties of HDRB

Particulars	Specifications
Cross-section (mm^2)	650×650
The rubber layer number	6
A rubber layer thickness (mm)	13.54
A steel layer thickness (mm)	2.3
Shear Modulus (Mpa)	1.2

In this analysis, the bridge superstructure is considered a horizontal rigid diaphragm, all the isolators experience the same displacement and therefore can be lumped into a single equivalent isolation

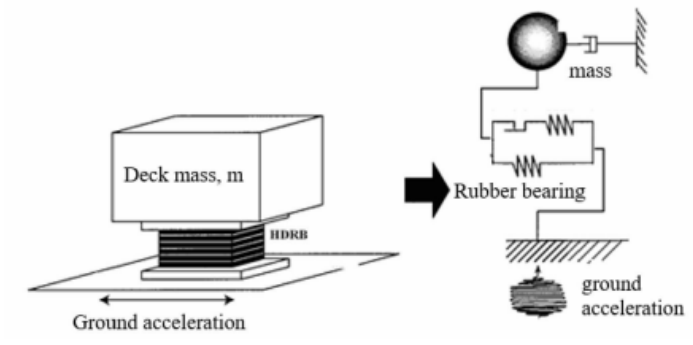

Figure 1. The model of the single degree of freedom system for the bridge's pier

unit, the superstructure of bridge is simulated as a mass, m, the vertical displacement of mass is eliminated. Then the bridge pier can be simply modeled as a single degree of freedom system (SDOF). The rubber bearing is assumed to be rigidly bonded to the substructure of bridges. The link between the superstructure and the mass m is HDRB as Fig. 1. In this paper, HDRB is modeled by the bilinear model in [4, 7] and the rheology model proposed by authors [8]. The comparison results will show the modeling effect of HDRB on the prediction of seismic responses of the bridge piers.

In seismic design guides and specifications [4, 7], the elasto-plastic bilinear model is commonly used for modeling isolation bearings in nonlinear dynamic analyses. The correct modeling of the bridge is very necessary to predict the seismic responses of the bridges with HDRB. In particular, the modeling of HDRB is very important for the bridges used. The bilinear model is shown in Fig. 2.

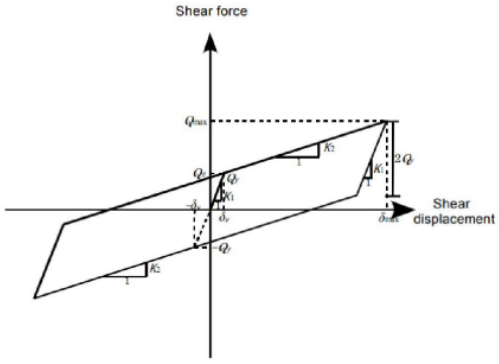

(a) Force-displacement relation

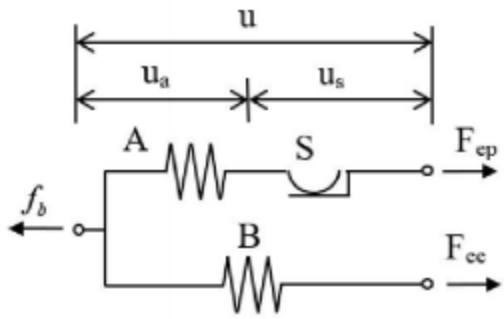

(b) Represented in a rheology model

Figure 2. Bilinear design model

The previous studies [9–14] have shown that the mechanical behavior of HDRB is strongly rate dependent with strain hardening at large levels. However, the design model in [4, 7] cannot reproduce this behavior of HDRB. In order to solve this limitation of the design model, the authors have proposed a rheology model of HDRB, which can reproduce the rate dependency behavior of HDRB in [8]. The proposed model is presented in Fig. 3.

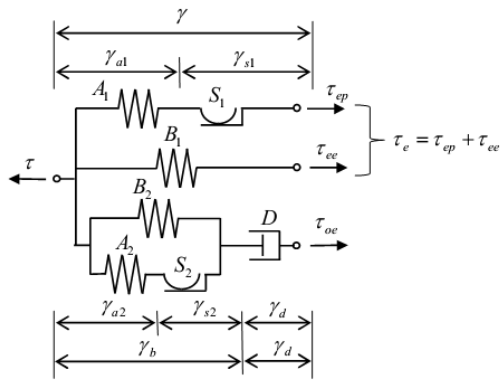

Figure 3. The proposed model in [8]

3. A numerical solution based on time-stepping Newmark's method

In this section, the motion equation of the SDOF system of the pier in Section 2 is solved by Newmark's method. For static analysis of the nonlinear SDOF system, the Newton-Raphson method is developed in this calculation. The resisting force fb of the motion equation is determined by two models: the bilinear model in [4, 7] and the proposed model in [8].

3.1. A numerical solution of the motion equation of SDOF system

The motion equation at the mass, m point of the SDOF system as

$$m\ddot{u} + c\dot{u} + f_b = p \tag{1}$$

where m is the mass of the upper structure and c is the damping coefficient of the upper structure. f_b is the resisting force of HDRB, p is an external force (earthquake), u is the horizontal displacement at the top of bearing.

a. Newton-Raphson Iteration

Considering a nonlinear equation to be solved in a static problem

$$f_S(u) = p \tag{2}$$

The objective is to determine the displacement u due to the external force p, where $f_S(u)$ has a nonlinear force-displacement relation.

Assume that after j cycles of iteration, $u^{(j)}$ is an estimate of the unknown displacement, and we will develop an iterative procedure. This procedure will provide an improved estimate of $u^{(j+1)}$.

$$(f_S)^{(j+1)} = (f_S)^{(j)} + \left.\frac{\partial f_S}{\partial u}\right|_{u^{(j)}} \left(u^{(j+i)} - u^{(j)}\right) + \frac{1}{2}\left.\frac{\partial^2 f_S}{\partial u^2}\right|_{u^{(j)}} \left(u^{(j+i)} - u^{(j)}\right)^2 + \ldots \tag{3}$$

If $u^{(j)}$ is near to the solution, to make change in u, $\Delta u^{(j)} = u^{(j+1)} - u^{(j)}$, will be very small and the second and higher order quantities can be ignored, leading to the linearized equation

$$(f_S)^{(j+1)} \approx (f_S)^{(j)} + k_T^{(j)} \Delta u^{(j)} = p \tag{4}$$

where $k_T^{(j)} = \left.\frac{\partial f_S}{\partial u}\right|_{u^{(j)}}$ is the tangent stiffness at $u^{(j)}$.

A residual force R is defined by the difference between the external force p and $f_S^{(j)}$

$$R^{(j)} = p - f_S^{(j)} = k_T^{(j)} \Delta u^{(j)} \tag{5}$$

The solution of the linear equation (5) is $\Delta u^{(j)}$ and an improved estimated displacement;

$$u^{(j+1)} = u^{(j)} + \Delta u^{(j)} \tag{6}$$

In order to check the solution in each iteration, and the repeat process will be stopped when the error's measure in the solution is smaller than a specified tolerance such as

$$\left|R^{(j)}\right| \leq \varepsilon_R \tag{7}$$

b. The time-stepping procedure based on Newmark's method

To develop Newton-Raphson iteration for dynamic analysis. The motion equation at the time $i+1$ step

$$\left(\hat{f}_S\right)_{i+1} = p_{i+1} \tag{8}$$

where

$$\left(\hat{f}_S\right)_{i+1} = m\ddot{u}_{i+1} + c\dot{u}_{i+1} + (f_b)_{i+1} \tag{9}$$

with u_{i+1}, $\dot{u}_{i+1}$, $\ddot{u}_{i+1}$ will be determined at time $i+1$ step.

The dynamic analysis Eq. (8) has the same form as the static analysis Eq. (2). So, we can apply the Taylor series expansion for Eq. (8), interpret $\left(\hat{f}_S\right)_{i+1}$ as a function of u_{i+1} as

$$\left(\hat{f}_S\right)_{i+1}^{(j+1)} \approx \left(\hat{f}_S\right)_{i+1}^{(j)} + \frac{\partial \hat{f}_S}{\partial u_{i+1}} \Delta u^{(j)} = p_{i+1} \tag{10}$$

where $\Delta u^{(j)} = u_{i+1}^{(j+1)} - u_{i+1}^{(j)}$.

Differentiating Eq. (9) at the known displacement $u_{i+1}^{(j)}$ to define the tangent stiffness

$$\left(\hat{k}_T\right)_{i+1}^{(j)} = \frac{\partial \hat{f}_S}{\partial u_{i+1}} = m\frac{\partial \ddot{u}}{\partial u_{i+1}} + c\frac{\partial \dot{u}}{\partial u_{i+1}} + \frac{\partial f_b}{\partial u_{i+1}} \tag{11}$$

The difference between the external force p_{i+1} and $\left(\hat{f}_S\right)_{i+1}^{(j)}$ is defined as the residual force $R_{i+1}^{(j)}$

$$R_{i+1}^{(j)} = p_{i+1} - \left(\hat{f}_S\right)_{i+1}^{(j)} = \left(\hat{k}_T\right)_{i+1}^{(j)} \Delta u^{(j)} \tag{12}$$

A family of time-stepping methods are developed Newmark, these methods are based on the following equations

$$u_{i+1} = u_i + (\Delta t)\,\dot{u}_i + (0.5-\beta)\,\Delta t^2 \ddot{u}_i + \beta \Delta t^2 \ddot{u}_{i+1} \tag{13}$$

$$\dot{u}_{i+1} = \dot{u}_i + (1-\gamma)\,\Delta t \ddot{u}_i + (\gamma \Delta t)\,\ddot{u}_{i+1} \tag{14}$$

From Eq. (13), $\ddot{u}_{i+1}$ can be expressed in terms of u_{i+1}

$$\ddot{u}_{i+1} = \frac{1}{\beta \Delta t^2}\left(u_{i+1} - u_i\right) - \frac{1}{\beta \Delta t}\dot{u}_i - \left(\frac{1}{2\beta} - 1\right)\ddot{u}_i \tag{15}$$

Substitute Eq. (15) into Eq. (14), $\dot{u}_{i+1}$ can be expressed in terms of u_{i+1}

$$\dot{u}_{i+1} = \frac{\gamma}{\beta \Delta t}\left(u_{i+1} - u_i\right) + \left(1 - \frac{\gamma}{\beta}\right)\dot{u}_i + \Delta t\left(1 - \frac{\gamma}{2\beta}\right)\ddot{u}_i \tag{16}$$

To differentiate Eq. (15) and (16)

$$\begin{cases} \dfrac{\partial \ddot{u}}{\partial u_{i+1}} = \dfrac{1}{\beta \Delta t^2} \\ \dfrac{\partial \dot{u}}{\partial u_{i+1}} = \dfrac{\gamma}{\beta \Delta t} \end{cases} \tag{17}$$

Substitute Eq. (17) into Eq. (11) to obtain the tangent stiffness $\left(\hat{k}_T\right)_{i+1}^{(j)}$

$$\left(\hat{k}_T\right)_{i+1}^{(j)} = \frac{1}{\beta \Delta t^2} m + \frac{\gamma}{\beta \Delta t} c + \left(k_T\right)_{i+1}^{(j)} \tag{18}$$

where $\left(k_T\right)_{i+1}^{(j)}$ is the bearing's stiffness.

Substitute Eq. (15) and (16) into Eq. (9) then substitute $\left(\hat{f}_S\right)_{i+1}^{(j)}$ into Eq. (12) to obtain the residual force $R_{i+1}^{(j)}$.

$$\begin{aligned} R_{i+1}^{(j)} = {} & p_{i+1} - \left(f_b\right)_{i+1}^{(j)} - \left(\frac{1}{\beta \Delta t^2} m + \frac{\gamma}{\beta \Delta t} c\right)\left(u_{i+1}^{(j)} - u_i\right) + \left[\frac{1}{\beta \Delta t} m + \left(\frac{\gamma}{\beta} - 1\right) c\right]\dot{u}_i \\ & + \left[\left(\frac{1}{2\beta} - 1\right) m + \Delta t\left(\frac{\gamma}{2\beta} - 1\right) c\right]\ddot{u}_i \end{aligned} \tag{19}$$

The bearing force $(f_b)_{i+1}^{(j)}$ and bearing stiffness$(k_T)_{i+1}^{(j)}$ can be obtained by the above two models. The seismic analysis based on time-stepping calculation procedure is described in Fig. 4.

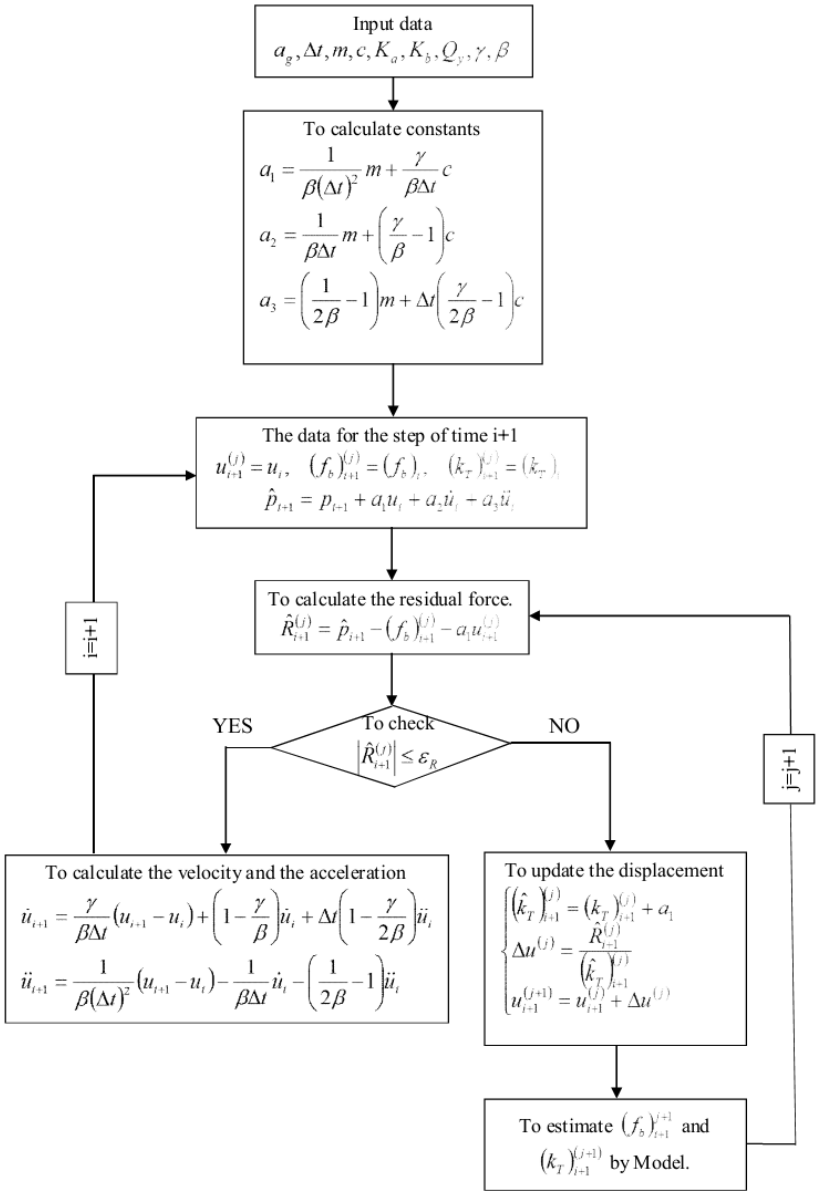

Figure 4. The chart to calculate the dynamic response of a SDOF system

c. The resisting force determined from models

• Bilinear model

The bearing force of $(f_b)_{i+1}^{(j)}$ is calculated by using the bilinear model in [4, 7]. The design model of the bearings is represented in a rheology model in Fig. 4.

$$f_b = F_{ep} + F_{ee} \tag{20}$$

where F_{ep} and F_{ee} are shown in Fig. 4(b).

The second branch in the Fig. 4 presents the elastic force F_{ee}

$$F_{ee} = K_b u \tag{21}$$

where K_b is the stiffness of spring B.

The first branch in Fig. 4 shows the elasto-plastic force F_{ep}

+ Spring A is linear:

$$F_{ep} = K_a u_a \tag{22}$$

where K_a is the stiffness of spring A.

+ If F_{ep} equals the yield force Q_y, the slider S will be activated and start to slide

$$\begin{cases} \dot{u}_s \neq 0 & \text{if} \quad \left|F_{ep}\right| = Q_y \\ \dot{u}_s = 0 & \text{if} \quad \left|F_{ep}\right| < Q_y \end{cases} \tag{23}$$

where Q_y is yield force.

To find the solution of Fep in the first branch, we will use a predicted calculation:

+ The F_{ep} and displacement relation is presented in Fig. 5.

+ To increase the displacement Δu_{i+1} as

$$\Delta u_{i+1} = u_{i+1} - u_i \tag{24}$$

+ The increment of F_{ep} in the bilinear model as

$$\Delta F_{ep,i+1} = K_a \Delta u_{i+1} \tag{25}$$

$$\Rightarrow F_{ep,i+1} = F_{ep,i} + \Delta F_{ep,i+1} \tag{26}$$

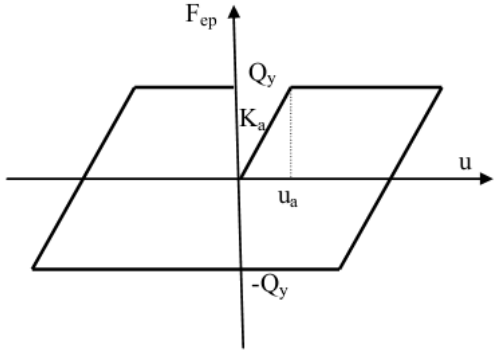

Figure 5. The force and displacement relation in the first branch

+ If $\left|F_{ep,i+1}\right| \geq Q_y$ as in Fig. 6(b)

$$F_{ep,i+1} = Q_y sign\left(\Delta u_{i+1}\right) \tag{27}$$

and

$$(k_T)_{i+1} = K_b \quad \text{if} \quad F_{ep,i+1}\Delta u_{i+1} > 0 \tag{28}$$

$$(k_T)_{i+1} = K_a + K_b \quad \text{if} \quad F_{ep,i+1}\Delta u_{i+1} < 0 \tag{29}$$

+ If $\left|F_{ep,i+1}\right| < Q_y$ as in Fig. 6(c)

$$F_{ep,i+1} = F_{ep,i+1} \tag{30}$$

and

$$(k_T)_{i+1} = K_a + K_b \tag{31}$$

The flow chart describes to calculate the bearing force $(f_b)_{i+1}$ and determine the tangent stiffness of the bearing $(k_T)_{i+1}$ at time i+1 step in Fig. 7.

In this analysis, the parameters of the bilinear model are determined in Nguyen et al. [15] for the room temperature case.

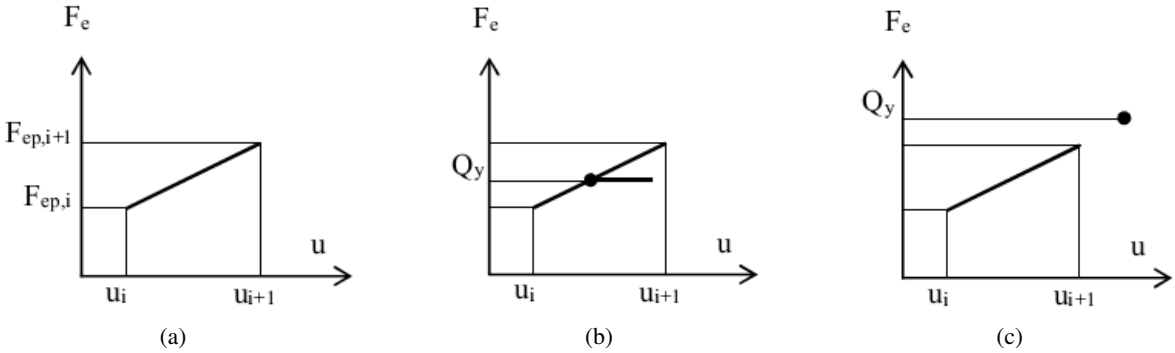

Figure 6. The method to predict the value of F_{ep} at step $i + 1$

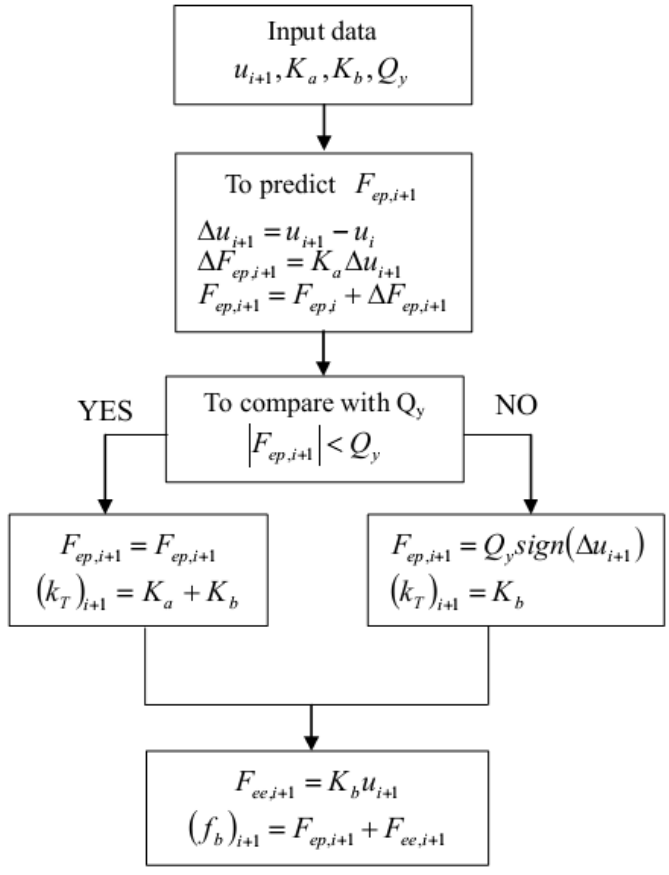

Figure 7. The flow chart describes to calculate the bearing force at the time $i + 1$ step

• Rheology model

In order to improve the bilinear model in producing the rate-dependent behavior of HDRB, the authors propose a rheology model in [8] as Fig. 3. The rheology model is used to determine the resisting force (bearing force) in this part;

* Representation of rate-independent equilibrium stresses in the first and second branches

- Spring A_1 is defined as

$$\tau_{ep} = C_1^{(EQ)}\gamma_{a1} \tag{32}$$

- Slider S_1 is defined as

$$\begin{cases} \dot{\gamma}_{s1} \neq 0 & \text{for} \quad \left|\tau_{ep}\right| = \tau_{cr}^{(EQ)} \\ \dot{\gamma}_{s1} = 0 & \text{for} \quad \left|\tau_{ep}\right| < \tau_{cr}^{(EQ)} \end{cases} \tag{33}$$

- Spring B_1 is defined as

$$\tau_{ee} = C_2^{(EQ)}\gamma + C_3^{(EQ)}|\gamma|^m \text{sgn}(\gamma) \tag{34}$$

$$\text{sgn}(x) = \begin{cases} +1 & : \quad x > 0 \\ 0 & : \quad x = 0 \\ -1 & : \quad x < 0 \end{cases} \tag{35}$$

- Solution of τ_{ep} in the first branch is obtained by a predicted calculation

$$\Delta\gamma_{i+1} = \gamma_{i+1} - \gamma_i \Rightarrow \Delta\tau_{ep,i+1} = C_1^{(EQ)}\Delta\gamma_{i+1} \Rightarrow \tau_{ep,i+1} = \tau_{ep,i} + \Delta\tau_{ep,i+1} \tag{36}$$

If

$$\left|\tau_{ep,i+1}\right| \geq \tau_{cr}^{(EQ)} \Rightarrow \Delta\tau_{ep,i+1} = \tau_{cr}^{(EQ)} sign\left(\Delta\gamma_{i+1}\right) - \tau_{ep,i}; \Delta\gamma_{a1,i+1} = \Delta\tau_{ep,i+1}/C_1^{(EQ)} \tag{37}$$

Else

$$\Rightarrow \Delta\tau_{ep,i+1} = \Delta\tau_{ep,i+1}; \quad \Delta\gamma_{a1,i+1} = \Delta\gamma_{i+1} \tag{38}$$

End

$$\tau_{ep,i+1} = \tau_{ep,i} + \Delta\tau_{ep,i+1} \tag{39}$$

$$\gamma_{a1,i+1} = \gamma_{a1,i} + \Delta\gamma_{a1,i+1} \tag{40}$$

* Representation of rate-dependent overstressed in the third branch

- Spring A_2 is defined as

$$\tau_a = C_1^{(OE)}\gamma_{a2} \tag{41}$$

- Element S_2 is defined as

$$\begin{cases} \dot{\gamma}_{s2} \neq 0 & \text{for} \quad |\tau_a| = \tau_{cr}^{(OE)} \\ \dot{\gamma}_{s2} = 0 & \text{for} \quad |\tau_a| < \tau_{cr}^{(OE)} \end{cases} \tag{42}$$

- Spring B_2 is defined as

$$\tau_b = C_2^{(OE)}\gamma_b \tag{43}$$

- The stress of D is presented:

$$\tau_{oe} = a|\dot{\gamma}_d|^n \text{sgn}\left(\dot{\gamma}_d\right) \tag{44}$$

- Solution of τ_{oe} in the third branch

+ To apply Euler's formula for differential equation (39), the expression for $\gamma_{d,i+1}$ can be obtained as

$$\gamma_{d,i+1} = \gamma_{d,i} + \Delta t \frac{\left|\tau_{oe,i}\right|^{1/n}}{a^{1/n}} sign\left(\tau_{oe,i}\right) \tag{45}$$

$$\Rightarrow \gamma_{b,i+1} = \gamma_{i+1} - \gamma_{d,i+1} \tag{46}$$

+ $\tau_{b,i+1}$ in spring B_2 is calculated by Eq. (38) from $\gamma_{b,i+1}$

+ $\tau_{a,i+1}$ in spring A_2 can be obtained by the predicted calculation that is the same calculation of $\tau_{ep,i+1}$ in the first branch.

$$\Delta\gamma_{b,i+1} = \gamma_{b,i+1} - \gamma_{b,i} \Rightarrow \Delta\tau_{a,i+1} = C_1^{(OE)}\Delta\gamma_{b,i+1} \Rightarrow \tau_{a,i+1} = \tau_{a,i} + \Delta\tau_{a,i+1} \tag{47}$$

If

$$\left|\tau_{a,i+1}\right| \geq \tau_{cr}^{(OE)} \Rightarrow \Delta\tau_{a,i+1} = \tau_{cr}^{(OE)}\,\text{sign}\left(\Delta\gamma_{b,i+1}\right) - \tau_{a,i}; \Delta\gamma_{a2,i+1} = \Delta\tau_{a,i+1}/C_1^{(OE)} \tag{48}$$

Else

$$\Rightarrow \Delta\tau_{a,i+1} = \Delta\tau_{a,i+1}; \quad \Delta\gamma_{a2,i+1} = \Delta\gamma_{b,i+1} \tag{49}$$

End

$$\tau_{a,i+1} = \tau_{a,i} + \Delta\tau_{a,i+1}; \quad \gamma_{a2,i+1} = \gamma_{a2,i} + \Delta\gamma_{a2,i+1} \tag{50}$$

+ $\tau_{oe,i+1}$ is the sum of $\tau_{a,i+1}$ and $\tau_{b,i+1}$

$$\tau_{oe,i+1} = \tau_{a,i+1} + \tau_{b,i+1} \tag{51}$$

* The bearing force and tangent stiffness of the bearing at time $i + 1$
- Total bearing stress:

$$\tau_{i+1} = \tau_{ep,i+1} + \tau_{ee,i+1} + \tau_{oe,i+1} \tag{52}$$

- To differentiate Eq. (44) at γ_{i+1}

$$\frac{\partial\tau_{i+1}}{\partial\gamma_{i+1}} = \frac{\partial\tau_{ep,i+1}}{\partial\gamma_{i+1}} + \frac{\partial\tau_{ee,i+1}}{\partial\gamma_{i+1}} + \frac{\partial\tau_{oe,i+1}}{\partial\gamma_{i+1}} \tag{53}$$

From Eq. (33)

$$\frac{\partial\tau_{ee,i+1}}{\partial\gamma_{i+1}} = C_2^{(OE)} + C_3^{(OE)}m|\gamma|^{m-1}\text{sign}\left(\gamma\right) \tag{54}$$

$$\begin{cases} \dfrac{\partial\tau_{eo,i+1}}{\partial\gamma_{i+1}} \approx \dfrac{\Delta\tau_{ep,i+1}}{\Delta\gamma_{i+1}} \\ \dfrac{\partial\tau_{oe,i+1}}{\partial\gamma_{i+1}} \approx \dfrac{\Delta\tau_{oe,i+1}}{\Delta\gamma_{i+1}} \end{cases} \tag{55}$$

With $\Delta\tau_{ep,i+1} = \tau_{ep,i+1} - \tau_{ep,i}; \Delta\tau_{oe,i+1} = \tau_{oe,i+1} - \tau_{oe,i}; \Delta\gamma_{i+1} = \gamma_{i+1} - \gamma_i$
- To differentiate Eq. (44) at $\dot{\gamma}_{i+1}$

$$\frac{\partial\tau_{i+1}}{\partial\dot{\gamma}_{i+1}} = \frac{\partial\tau_{ep,i+1}}{\partial\dot{\gamma}_{i+1}} + \frac{\partial\tau_{ee,i+1}}{\partial\dot{\gamma}_{i+1}} + \frac{\partial\tau_{oe,i+1}}{\partial\dot{\gamma}_{i+1}} = \frac{\partial\tau_{oe,i+1}}{\partial\dot{\gamma}_{i+1}} \tag{56}$$

Because τ_{ep} and τ_{ee} are rate-independent.
From

$$\gamma_d = \gamma - \gamma_b \quad \Rightarrow \quad \dot{\gamma}_d = \dot{\gamma} - \dot{\gamma}_b \tag{57}$$

- Substitute Eq. (48) into Eq. (39) and differentiate Eq. (39)

$$\begin{aligned} \frac{\partial\tau_{i+1}}{\partial\dot{\gamma}_{i+1}} = \frac{\partial\tau_{oe,i+1}}{\partial\dot{\gamma}_{i+1}} &= a\frac{\partial\left(|\dot{\gamma} - \dot{\gamma}_b|^n\right)}{\partial\left(\dot{\gamma}\right)}sign\left(\dot{\gamma} - \dot{\gamma}_b\right) + a|\dot{\gamma} - \dot{\gamma}_b|^n\frac{\partial\left(sign\left(\dot{\gamma} - \dot{\gamma}_b\right)\right)}{\partial\left(\dot{\gamma}\right)} \\ &= an|\dot{\gamma} - \dot{\gamma}_b|^{n-1}sign\left(\dot{\gamma} - \dot{\gamma}_b\right) + a|\dot{\gamma} - \dot{\gamma}_b|^n 2dirac\left(\dot{\gamma} - \dot{\gamma}_b\right) \end{aligned} \tag{58}$$

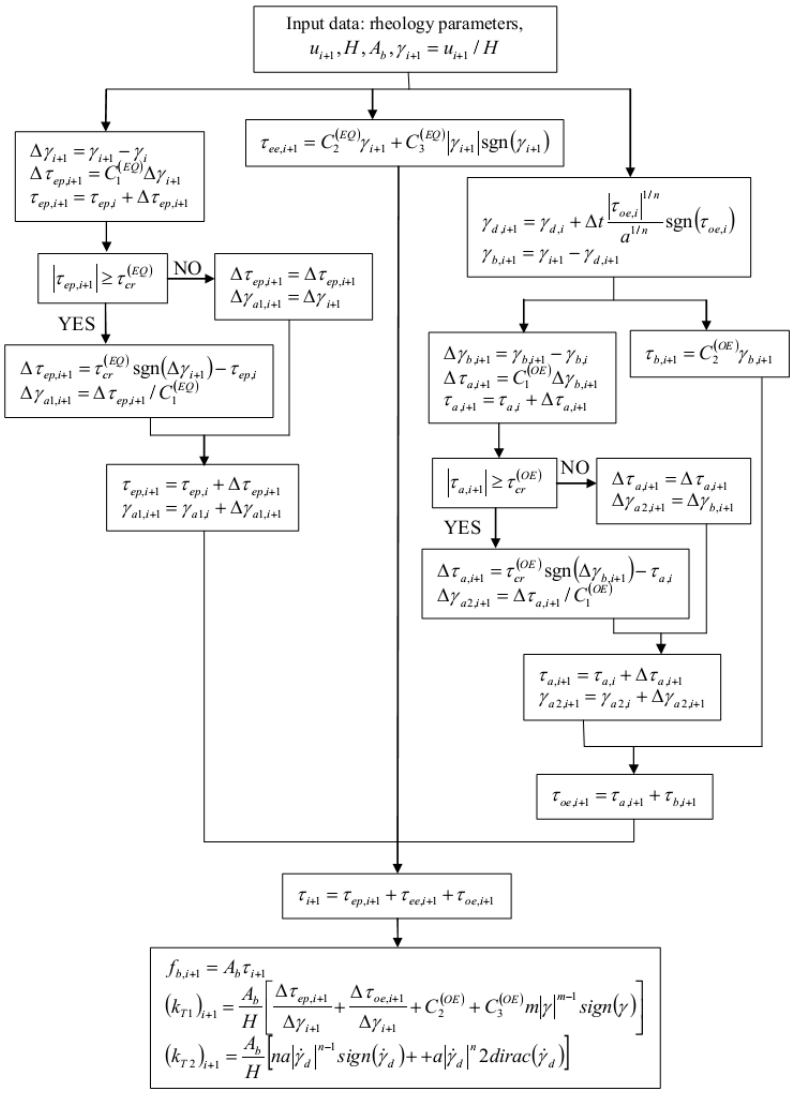

Figure 8. The flow chart describes to calculate the bearing force and the bearing stiffness at time $i + 1$

$$\Rightarrow \frac{\partial\tau_{i+1}}{\partial\dot{\gamma}_{i+1}} = na|\dot{\gamma}_d|^{n-1}sign\,(\dot{\gamma}_d) + a|\dot{\gamma}_d|^n 2dirac\,(\dot{\gamma}_d) \tag{59}$$

- The bearing force at time $i + 1$

$$f_{b,i+1} = A_b\tau_{i+1} \tag{60}$$

where A_b is the cross-section of the bearing

- The tangent stiffness at time $i + 1$

$$(k_{T1})_{i+1} = \frac{\partial f_{b,i+1}}{\partial u_{i+1}} = \frac{\partial\,(A_b\tau_{i+1})}{\partial\,(H\gamma_{i+1})} = \frac{A_b\partial\tau_{i+1}}{H\partial\gamma_{i+1}} \tag{61}$$

$$(k_{T2})_{i+1} = \frac{\partial f_{b,i+1}}{\partial\dot{u}_{i+1}} = \frac{\partial\,(A_b\tau_{i+1})}{\partial\,(H\dot{\gamma}_{i+1})} = \frac{A_b\partial\tau_{i+1}}{H\partial\dot{\gamma}_{i+1}} \tag{62}$$

where H is the total rubber thickness

- Substitute Eq. (46) into Eq. (51a)

$$(k_{T1})_{i+1} = \frac{A_b}{H}\left[\frac{\Delta\tau_{ep,i+1}}{\Delta\gamma_{i+1}} + \frac{\Delta\tau_{oe,i+1}}{\Delta\gamma_{i+1}} + C_2^{(OE)} + C_3^{(OE)} m|\gamma|^{m-1} sign(\gamma)\right] \tag{63}$$

- Substitute Eq. (49b) into Eq. (51b)

$$(k_{T2})_{i+1} = \frac{A_b}{H}\left[na|\dot{\gamma}_d|^{n-1} sign(\dot{\gamma}_d) + a|\dot{\gamma}_d|^n 2dirac(\dot{\gamma}_d)\right] \tag{64}$$

The flow chart describes the bearing force and the tangent stiffness of bearings by the rheology model in Fig. 9. The rheology model parameters in this paper are the same as the parameters of the model in [8] at 23 °C.

Based on the flow chart in Figs. 4, 7, 8, a program is developed and an algorithm is implemented in Matlab software [5]. The seismic responses at the top of the bearing are obtained by this program.

d. Input data of the dynamics analysis

The bridge and bearings used in this analysis are similar to [6]. However, the rubber bearings are HDRB, the bearings in [6] are nature rubber bearings and lead rubber bearings. The area of HDRB is A_b of 0.65×0.65 m^2. Total rubber thickness is H of $6 \times 0.01354 = 0.08124$ m. The steel girders, covered asphalt, reinforced concrete slab, and rail are superstructures. The mass of the structure is calculated for P1 pier with a span of 35.0 meters, $M = 196928$ (kg). The viscous damping of the structure is h of 5%. The natural period is T of 2 sec for the type II earthquake [4]. The structure's damping coefficient, $C = 2hM\omega = 2hM\frac{2\pi}{T}$ (N.s/m). Time integration step: $\Delta t = 0.01$ (s); $\gamma = 1/2$, and $\beta = 1/6$. The tolerance of residual force is ε_R of $0.001 \times Q_y$ (N). Earthquake ground motion in Fig. 9.

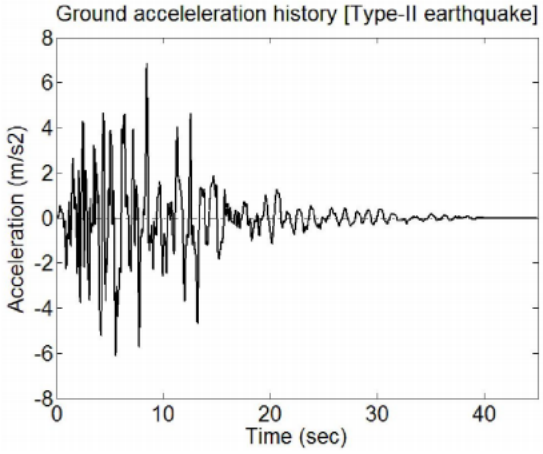

Figure 9. The type-II earthquake

3.2. The seismic responses at the top of the bearings obtained from the solution

The difference is very clear in Figs. 10 and 11. It means that the bridge's seismic responses strongly depend on the modeling approach of HDRB used in the bridge. Therefore, the engineers have to be careful to choose the model for HDRB in the practice design.

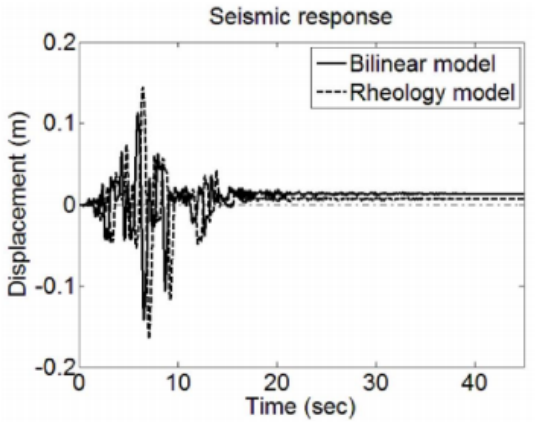

Figure 10. Displacement responses

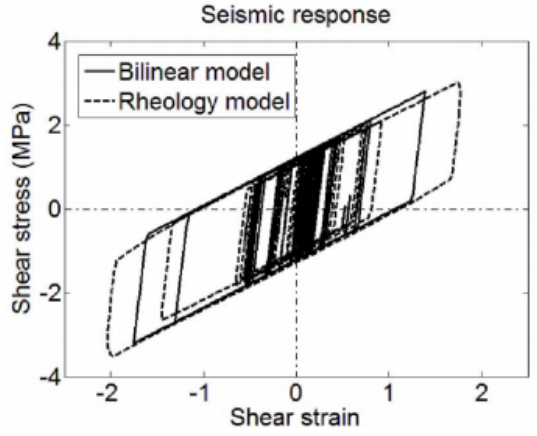

Figure 11. Stress-strain responses

4. Conclusions

A numerical solution has been successfully developed for determining the seismic hysteresis loops of HDRB at the top of the bridge pier. The motion equation of the nonlinear SDOF system of the piers is solved by Newmark's method. The iteration Newton-Raphson method is also employed in this calculation for static analysis of the nonlinear system. HDRB of the pier is modeled by the two models: the bilinear design model and the proposed rheology model. After that, the comparing results obtained from the two models show that the seismic hysteresis loops strongly depend on the modeling of HDRB. This is the important note for engineers to design the earthquake resistance of bridges using HDRB.

References

[1] Chopra, A. K. (2012). *Dynamics of structures: theory and application to earthquake engineering*. 4th edition, Prentice Hall, Englewood, New Jersey.

[2] Bhuiyan, A. R. (2009). Rheology modeling of laminated rubber bearings for seismic analysis. PhD thesis, Saitama University, Japan.

[3] Naeim, F., Kelly, J. (1996). *Design of seismic isolated structures*. 1st edition, John Wiley and Sons, New York.

[4] Japan Road Association (JRA) (2004). *Bearing support design guide for highway bridges*. Tokyo: Maruzen.

[5] Brian R., H., Tonald L., L., Jonathan M. R. Kevin R., C., John E., O., Garrent J., S. (2001). *A Guide to MATLAB for Beginners and Experienced Users*. Cambridge University Press, New York.

[6] Razzaq, M. K., Okui, Y., Bhuiyan, A. R., Amin, A. F. M. S., Mitamura, H., Imai, T. (2012). Application of rheology modeling to natural rubber and lead rubber bearings : a simplified model and low temperature behavior. *Journal of Japan Society of Civil Engineers, Ser. A1 (Structural Engineering & Earthquake Engineering (SE/EE))*, 68(3):526–541.

[7] American Association of State Highways and Transportation Officials (AASHTO) (2000). *Guide specification for seismic isolation design*. 2nd edition, Washington D.C., USA.

[8] Nguyen, D. A., Dang, J., Okui, Y., Amin, A. F. M. S., Okada, S., Imai, T. (2015). An improved rheology model for the description of the rate-dependent cyclic behavior of high damping rubber bearings. *Soil Dynamics and Earthquake Engineering*, 77:416–431.

[9] Abe, M., Yoshida, J., Fujino, Y. (2004). Multiaxial behaviors of laminated rubber bearings and their modeling. II: Modeling. *Journal of Structural Engineering*, 130(8):1133–1144.

[10] Bhuiyan, A. R., Okui, Y., Mitamura, H., Imai, T. (2009). A rheology model of high damping rubber bearings for seismic analysis: Identification of nonlinear viscosity. *International Journal of Solids and Structures*, 46(7-8):1778–1792.

[11] Dall'Asta, A., Ragni, L. (2006). Experimental tests and analytical model of high damping rubber dissipating devices. *Engineering Structures*, 28(13):1874–1884.

[12] Hwang, J. S., Wu, J. D., Pan, T.-C., Yang, G. (2002). A mathematical hysteretic model for elastomeric isolation bearings. *Earthquake Engineering & Structural Dynamics*, 31(4):771–789.

[13] Kikuchi, M., Aiken, I. D. (1997). An analytical hysteresis model for elastomeric seismic isolation bearings. *Earthquake Engineering & Structural Dynamics*, 26(2):215–231.

[14] Tsai, C. S., Chiang, T.-C., Chen, B.-J., Lin, S.-B. (2003). An advanced analytical model for high damping rubber bearings. *Earthquake Engineering & Structural Dynamics*, 32(9):1373–1387.

[15] Dung, N. A., Chuong, N. T., Okui, Y. (2016). *Effect of self-heating of high damping rubber bearings on design practice*. Canada-Japan-Vietnam Workshop on Composites, August 8-10/8/ 2016, Ho Chi Minh City, Vietnam.